

# Gabor Wavelet Networks for Object Representation and Face Recognition

Volker Krüger and Gerald Sommer

Computer Science Institute, Christian-Albrechts University Kiel  
Preußerstr. 1-9, 24105 Kiel, Germany  
Tel: ++49-431-560496, FAX: ++49-431-560481  
email: vok@ks.informatik.uni-kiel.de

**Abstract.** The choice of the object representation is crucial for an effective performance of cognitive tasks such as object recognition, fixation, etc. In this paper we want to introduce the Gabor wavelet network for an effective object representation. The Gabor wavelet network has several advantages such as invariance to some degree with respect to translation, rotation and dilation. Furthermore, it has the ability to generalize and to abstract from the training data and to assure, for a given network size, that a maximum of object information is coded. We will show in the experiments how Gabor wavelet networks can be used for face recognition applications.

**Keywords:** Gabor wavelets, object representation, face recognition

## 1 Introduction

It is a crucial question how object information, or image information in general, should be represented for cognitive systems to perform effectively, because it is the representation that decides on the distance and similarity measurements. When dealing with digital images most types of representations that encode the image information result in a data reduction and it is again the type of information representation that decides which image information is relevant, i.e. is encoded, and which is not. Other important topics in this context are invariance properties and the question, whether the information is encoded globally or locally. For example, principle component analysis [10], which is very often applied in face recognition problems, has no invariance with respect to translation, rotation or scale. Also information is encoded globally, which means that for example an image is always taken as a whole and local changes in the image result in a large global change of the representation. On the other hand, the bunch graph approach [13], a very successful representation approach for face recognition, is invariant to some degree with respect to translation, rotation and scale. In this approach the information is represented locally, which means that a local change in the image results in a local change in the representation. Another aspect is that the type of information representation decides on the possibility to abstract from the image data to a possibly symbolic representation of an object.

In this paper we want to present an object representation that is based on Gabor wavelet networks and superwavelets. Gabor wavelet networks have several advantages: by their very nature, Gabor wavelet networks (GWNs) are invariant to some degree to affine deformations and illumination changes. Furthermore, GWNs represent object features in a local manner, and unlike the discrete wavelet representation, the Gabor wavelet network uses wavelets whose parameters are chosen from a *continuous* parameter space (the phase space). This allows each wavelet to adapt its scale, orientation and position optimally to the structure of the object on which the wavelet network is trained. This ensures, by using a given number of Gabor wavelets, that a maximum of image information is preserved. For object recognition purposes this is the most important aspect.

A GWN has further conceptual advantages: using a small number of Gabor wavelets, the GWN is capable to generalize. As more and more Gabor wavelets are used, the GWN becomes more and more specific. In this sense the GWN behaves like an RBF network, that allows a generalization of the training data to some degree while using only a small set of basis functions. As the number of basis functions increases, the RBF network becomes overtrained, and so does the GWN.

The GWN even seems to allow an abstraction hierarchy. An abstraction hierarchy implies that the image can be considered as an expansion into image primitives, which can be viewed as conceptual building blocks forming the image [4]. This gives rise to the hope that one might find a symbolic representation of an object that is represented by a GWN.

In the following section we will give an extensive introduction to GWNs. Also, we will discuss each single point mentioned above, including the invariance properties, the generalization capability, the abstraction capability and the specificity of the wavelet parameters for the object representation. In the experimental section we will show how GWNs can be used for face recognition. In the last section we will conclude with some final remarks.

## 2 Introduction to Gabor Wavelet Networks

In this section we want to propose, as a major contribution of this work, the Gabor Wavelet Network for image representation. The idea of the wavelet network is inspired by [15], and the use of Gabor functions is inspired by the fact that they provide the best possible trade off between spatial resolution and frequency resolution. Furthermore, the Gabor filters are recognized to be good feature detectors [9]. An image representation with Gabor Wavelet Networks has the advantage of being sparser than the Gabor jet representation [13]. Yet, it allows to encode almost the entire image information and allows a good reconstruction.

To define a GWN, we start out, generally speaking, by taking a family of  $N$  odd Gabor wavelet functions  $\Psi = \{\psi_{\mathbf{n}_1}, \dots, \psi_{\mathbf{n}_N}\}$  of the form

$$\begin{aligned} \psi_{\mathbf{n}}(x, y) = & \exp \left( -\frac{1}{2} \left[ s_x \left( (x - c_x) \cos \theta - (y - c_y) \sin \theta \right) \right]^2 \right. \\ & \left. + \left[ s_y \left( (x - c_x) \sin \theta + (y - c_y) \cos \theta \right) \right]^2 \right) \\ & \times \sin \left( s_x \left( (x - c_x) \cos \theta - (y - c_y) \sin \theta \right) \right) , \end{aligned} \quad (1)$$

with  $\mathbf{n} = (c_x, c_y, \theta, s_x, s_y)^T$ . Here,  $c_x, c_y$  denote the translation of the Gabor wavelet,  $s_x, s_y$  denote the dilation and  $\theta$  denotes the orientation. The parameters  $\mathbf{n}_i$  (translation, orientation and dilation) of the wavelets may be chosen arbitrarily at this point. According to [15], any function  $f \in \mathbb{L}^2(\mathbb{R}^2)$  can be represented by a wavelet network. We are therefore going to interpret the image  $f$  to be a function of the space  $\mathbb{L}^2(\mathbb{R}^2)$  and assume further, without loss of generality that  $f$  is DC-free. In order to find the GWN for image  $f$  we minimize the energy function

$$E = \min_{\mathbf{n}_i, w_i \text{ for all } i} \|f - \sum_i w_i \psi_{\mathbf{n}_i}\|_2^2 \quad (2)$$

with respect to the weights  $w_i$  and the wavelet parameters  $\mathbf{n}_i$ . Equation (2) says that the  $w_i$  and  $\mathbf{n}_i$  are optimized (i.e. translation, dilation and orientation of each wavelet are chosen) such that the image  $f$  is optimally approximated by the weighted sum of Gabor wavelets  $\psi_{\mathbf{n}_i}$ . We therefore define a Gabor wavelet network as follows:

**Definition:** Let  $\psi_{\mathbf{n}_i}, i = 1, \dots, N$  be a set of Gabor wavelets,  $f$  a DC-free image and  $w_i$  and  $\mathbf{n}_i$  chosen according to the energy function (2). The two vectors  $\Psi = (\psi_{\mathbf{n}_1}, \dots, \psi_{\mathbf{n}_N})^T$  and  $\mathbf{w} = (w_1, \dots, w_N)^T$  define then the *Gabor wavelet network*  $(\Psi, \mathbf{w})$  for image  $f$ .

The parameters  $\mathbf{n}_i$  are chosen from *continuous* phase space and the Gabor wavelets are positioned with sub-pixel accuracy. This is precisely the main advantage over the discrete approach [2; 8]. While in the case of a discrete phase space local image structure has to be approximated by a combination of wavelets, a *single* wavelet can be chosen selectively in the continuous case to reflect precisely the local image structure. This assures that a maximum of the image information is encoded. It also leads to an almost symbolic abstraction [4] of the image data, as we will see later.

Using the optimal wavelets  $\Psi$  and weights  $\mathbf{w}$  of the Gabor wavelet network of an image  $f$ ,  $f$  can be (closely) reconstructed by a linear combination of the weighted wavelets:

$$\hat{f} = \sum_{i=0}^N w_i \psi_{\mathbf{n}_i} = \Psi^T \mathbf{w} .$$



**Fig. 1.** The left image shows the original face image  $I$ , the center image shows its reconstruction  $\hat{I}$  using formula (3) with an optimal wavelet net  $\Psi$  of just  $N = 52$  odd Gabor wavelets, distributed over the inner face region. The right image shows the optimal positions of the first 16 Gabor wavelets.

Of course, the quality of the image representation and of the reconstruction depends on the number  $N$  of wavelets used. An example reconstruction can be seen in fig. 1:  $N = 52$  wavelets are distributed over the inner face region of the left image  $I$  by the minimization formula (2). The reconstruction  $\hat{I}$  with formula (3) is shown in the center image. Note that the Gabor wavelets are continuous functions that interpolate the discrete image they are trained on. This fact will be of great importance later when we need to deform  $\hat{I}$  affinely.

Minimizing equation (2) is crucial, because finding a global minimum is an inefficient task. In order to find a GWN ( $\Psi, \mathbf{w}$ ) for a discrete gray value image  $I$ , we use the Levenberg-Marquard gradient descent method [11]. This method might get stuck in local minima and a careful selection of the initial parameters is therefore important. We use prior knowledge about significant image features to allow a task oriented optimization.

## 2.1 Direct Calculation of Weights

Gabor wavelet functions are not orthogonal. For a given family  $\Psi$  of Gabor wavelets it is not possible to calculate a weight  $w_i$  directly by a simple projection of the Gabor wavelet  $\psi_{\mathbf{n}_i}$  onto the image. In [2; 3] it was therefore proposed to use eq. (2) to find the optimal weight  $w_i$  for each fixed wavelet. Because optimization is a slow process, we want to suggest a direct calculation of the correct weights  $w_i$  by projecting the *dual* wavelets  $\tilde{\psi}_{\mathbf{n}_i}$ . The wavelet  $\tilde{\psi}_{\mathbf{n}_i}$  is the dual wavelet to the wavelet  $\psi_{\mathbf{n}_i}$  if  $\langle \psi_{\mathbf{n}_i}, \tilde{\psi}_{\mathbf{n}_j} \rangle = \delta_{i,j}$ . With  $\tilde{\Psi} = (\tilde{\psi}_{\mathbf{n}_1}, \dots, \tilde{\psi}_{\mathbf{n}_N})^T$ , we can write  $\left[ \langle \Psi, \tilde{\Psi} \rangle \right] = \mathbf{I}$  and we find  $\tilde{\psi}_{\mathbf{n}_i}$  to be  $\tilde{\psi}_{\mathbf{n}_i} = \sum_j (\Psi_{i,j})^{-1} \psi_{\mathbf{n}_j}$ , where  $(\Psi_{i,j}) = \langle \psi_i, \psi_j \rangle$ . This allows us to define the operator

$$\mathcal{T}_{\Psi} : \mathbb{L}^2(\mathbb{R}^2) \longrightarrow \mathbb{L}^2(\mathbb{R}^2)$$

as follows: Given a set  $\Psi$  of optimal wavelets of a GWN, trained on the function  $f$ , the operator  $\mathcal{T}_{\Psi}$  realizes an orthogonal projection of a function  $g$  onto the



**Fig. 2.** The figure shows images of a wooden toy block on which a GWN was trained. The black line segments sketch the positions, sizes and orientations of all the wavelets of the GWN (left), and of some automatically selected wavelets (right).

vector space that is spanned by  $\Psi$  (see (3)), i.e.

$$\hat{g} = \mathcal{T}_{\Psi}(g) = \sum_{i=1}^N w_i \psi_{\mathbf{n}_i} \text{ with } \mathbf{w} = \tilde{\Psi}g .$$

Clearly, by definition ( $\Psi$  is chosen optimal for  $f$ ),  $\mathcal{T}_{\Psi}(f) = \hat{f} \approx f$ . Furthermore, for any  $\epsilon > 0$  we find a network size  $N$  such that  $\|f - \mathcal{T}_{\Psi}(f)\|^2 < \epsilon$  and, because of the continuity of  $\mathcal{T}_{\Psi}$ , we also find for any  $\epsilon > 0$  a  $\delta$  such that  $\|(f + \delta) - \mathcal{T}_{\Psi}(f + \delta)\|^2 < \epsilon$ .

## 2.2 Symbolic Abstraction

Generally, two different types of hierarchies can be distinguished [4]:

- *scale hierarchies*
- *abstraction hierarchies.*

GWNs allow an abstraction hierarchy of the coded data to some degree [7]. An abstraction hierarchy implies that the image can be considered as an expansion into image primitives, such as line or edge segments, that can be viewed as conceptual building blocks forming the image [4]. In terms of an abstraction pyramid, we have the image itself at the first level, described as a combination of gray value pixels. At the higher 2nd level we have a description of line and edge elements. An example can be seen in fig. 2. The figure shows the image of a little wooden toy block, on which a Gabor wavelet network was trained. The left image shows the positions, scales and orientations of the wavelets as little black line segments. By thresholding the weights, the more “important” wavelets may be selected, which leads to the right image\*. The reason for the behavior of the Gabor wavelets in fig. 2 is clear: odd Gabor wavelet functions show their highest impulse response on edge segments that are of the same position and of the same orientation as the Gabor wavelet function itself. Ideally, each Gabor wavelet should be positioned exactly on the image line after optimization. Also its scale and orientation should reflect the scale and orientation of the image line. In reality, however, interactions with other wavelets of the network have to be considered so that the wavelet parameters reflect the position, scale, and orientation of the image line closely, but not precisely. This fact can clearly be seen in fig. 2.

\* Since the weights depend on the contrast of the image, they were normalized before selecting the ones with a weight  $> 0.8$ . It should be mentioned that this simple proceeding is possible only on images with clear edges.

### 2.3 Reparameterization Gabor Wavelet Networks

The “reverse” task of finding the position, the scale and the orientation of a GWN in a new image is most important. For example, consider an image  $J$  that shows the person of fig. 1, left, possibly distorted affinely. Given a corresponding GWN we are interested in finding the correct position, orientation and scaling of the GWN so that the wavelets are positioned on the same facial features as in the original image. An example for this can be seen in fig. 1, where in the right image the original positions of the wavelets are marked and in fig. 4, where in new images the wavelet positions of the *reparameterized* wavelet network are marked.

Parameterization of a wavelet net is established by using a *superwavelet* [12].

**Definition:** Let  $(\Psi, \mathbf{w})$  be a Gabor wavelet network with  $\Psi = (\psi_{\mathbf{n}_1}, \dots, \psi_{\mathbf{n}_N})^T$ ,  $\mathbf{w} = (w_1, \dots, w_N)^T$ . A *superwavelet*  $\Psi_{\mathbf{n}}$  is defined to be a linear combination of the wavelets  $\psi_{\mathbf{n}_i}$  such that

$$\Psi_{\mathbf{n}}(\mathbf{x}) = \sum_i w_i \psi_{\mathbf{n}_i}(\mathbf{S}\mathbf{R}(\mathbf{x} - \mathbf{c})), \quad (3)$$

where the parameters of vector  $\mathbf{n}$  of superwavelet  $\Psi$  define the dilation matrix  $\mathbf{S} = \text{diag}(s_x, s_y)$ , the rotation matrix  $\mathbf{R}$ , and the translation vector  $\mathbf{c} = (c_x, c_y)^T$ .

A superwavelet  $\Psi_{\mathbf{n}}$  is again a wavelet [12] and in particular a continuous function that has the wavelet parameters dilation, translation and rotation (see section 2). Therefore, we can handle it in the same way as we handled each single wavelet in the previous section. For a new image  $g$  we may arbitrarily deform the superwavelet by optimizing its parameters  $\mathbf{n}$  with respect to the energy function  $E$ :

$$E = \min_{\mathbf{n}} \|g - \Psi_{\mathbf{n}}\|_2^2 \quad (4)$$

Equation (4) defines the operator

$$\begin{aligned} \mathcal{P}_{\Psi} : \mathbb{L}^2(\mathbb{R}^2) &\longmapsto \mathbb{R}^5 \\ g &\longrightarrow \mathbf{n} = (c_x, c_y, \theta, s_x, s_y), \end{aligned} \quad (5)$$

where  $\mathbf{n}$  minimizes the energy function  $E$  of eq. (4). For optimization of the superwavelet parameters, we can elegantly use the same optimization procedure as in section 2. An example of the optimization process can be seen in fig. 3: Shown are the initial values of  $\mathbf{n}$ , the values after 2 and 4 optimization cycles and the final values after 8 cycles, each marked with the white square. The square refers to the inner face region. Its center position marks the center position of the corresponding superwavelet. The superwavelet used in fig. 3 is  $\hat{I}_4$  of fig. 1. A further example can be seen in fig. 4. The 1st and 3rd image have to be compared with the right image in fig. 1: It can be seen that the wavelets are positioned



**Fig. 3.** The images show the 1st, the 2th(top), the 4th and the 8th (final) step (bottom) of the gradient descent method optimizing the parameters of a superwavelet. The top left image shows the initial values with 10 px. off from the true position, rotated by  $10^\circ$  and scaled by 20%. The bottom right image shows the final result. As superwavelet,  $\hat{I}_4$  of figure 1 was used.

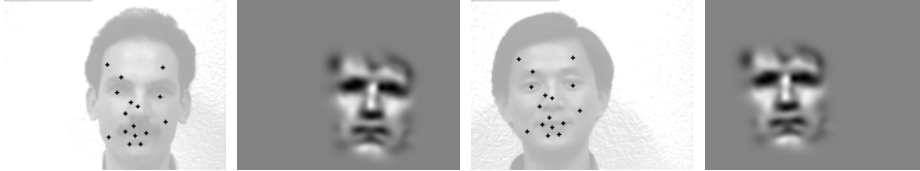


**Fig. 4.** The images show the positions of each of the 16 wavelets after reparameterizing the wavelet net (top) and the corresponding reconstruction (bottom). The reconstructed faces show the same orientation, position and size as the ones they were reparameterized on.

correctly on the same corresponding facial features (see fig. 1). The 2nd and 4th image of fig. 4 shows the reconstructions using the reparameterized GWNs.

The reparameterization of the superwavelet can be understood as warping, where the original face, represented by the GWN  $(\Psi, \mathbf{w})$  is warped onto the new face. This idea is shown in fig. 5.

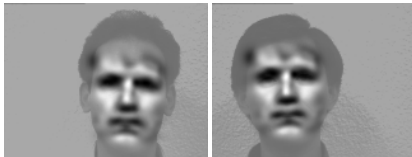


**Fig. 5.** The two images show the wavelet net  $\hat{I}_{4,6}$ , repositioned onto the two test images of fig. 4. This demonstrates that the repositioning process can be understood as warping the superwavelet onto the new test faces.

The reparameterization (warping) works quite robust: Using the superwavelet  $\hat{I}_4$  or  $\hat{I}_{4,6}$ , we have found in several experiments on the subjects in fig. 4 that the initialization of  $\mathbf{n}_0$  may vary from the correct parameters by approx.  $\pm 10$  px in  $x$  and  $y$  direction, by approx. 20% in scale and by approx.  $\pm 10^\circ$  in rotation (see fig. 3). Of course, these are only approximate values since they depend on the number of wavelets used, on the template face and on the scale of the used wavelets. In our case, 10 px. correspond to  $\approx 1/3$  of the width of the white box in fig. 3, marking the inner face region.

### 3 Face Recognition independent of Gesture

Various applications to Gabor Wavelet Networks have been discussed, among them affine real time face tracking [6] and efficient head pose estimation [5].

In this section we will present some promising face recognition results while using GWNs for the face representation. By training a GWN  $(\Psi, \mathbf{w})$  on an image  $f$  and applying the GWN to a test image  $g$ , the recognition is established in two steps:

1. optimal repositioning of the GWN by using the positioning operator  $\mathcal{P}_\Psi$
2. calculating the optimal weights for the optimally repositioned GWN by using the projection operator  $\mathcal{T}_\Psi$ .

This can be written concisely as

$$\mathcal{T}_\Psi^{\mathcal{P}(g)}(g) = \hat{g} \quad (6)$$

This composite operator leads to an image very similar to  $g$  if, and only if,  $g$  is well characterized by the GWN of the operator  $\mathcal{T}_\Psi$ . This means that (6) is approximately the identity, if, and only if,  $g \approx f$  or  $g = \mathbf{0}^{**}$  (images are assumed to be DC-free). Assuming, without loss of generality, that  $g \neq 0$ , we can write:

$$\mathcal{T}_\Psi^{\mathcal{P}(g)}(g) = \begin{cases} \hat{g} \approx g & \text{iff } g \approx f \\ \hat{g} \neq g & \text{iff } g \neq f \end{cases} \quad (7)$$

Using eq. (7) it is straight forward to define the following *distance measure*:

$$d_\Psi(f, g) = \|\mathcal{T}_\Psi^{\mathcal{P}(g)}(f) - \mathcal{T}_\Psi^{\mathcal{P}(g)}(g)\|_2^2 \quad (8)$$

The distance measurement  $d_\Psi(f, g)$  is defined to be the sum of squared differences between the wavelet representations of the training image  $f$  that is warped onto the test image  $g$ , which is  $\mathcal{T}_\Psi^{\mathcal{P}(g)}(f)$ , and the wavelet representation of the test image  $g$ ,  $\mathcal{T}_\Psi^{\mathcal{P}(g)}(g)$ , represented with the wavelet set  $\Psi$  of a GWN that was trained on image  $f$ . In fig. 6, an example is shown: the image  $\mathcal{T}_\Psi^{\mathcal{P}(g)}(f)$  (left), and the image  $\mathcal{T}_\Psi^{\mathcal{P}(g)}(g)$ (right). The distance  $d_\Psi$  is given to be the sum of squared differences between the two shown images. In the ideal case where



**Fig. 6.** The two images show the original image  $f$ , warped onto the image  $g$ ,  $\mathcal{T}_\Psi^{\mathcal{P}(g)}(f)$ , (left) and the result of the operator  $\mathcal{T}_\Psi^{\mathcal{P}(g)}$  applied on the image  $g$ . The distance  $d_\Psi(f, g)$  of images  $f, g$ , is defined to be the sum of squared differences between these two shown images.

the test image  $g$  is the same as the training image  $f$ , the  $d_\Psi$  distance should be zero. Note that with  $\mathcal{T}_\Psi^{\mathcal{P}(g)}(f)$  the wavelet representation of  $f$  is warped onto image  $g$  so that, when doing a pixel wise comparison of the two images, only corresponding image features are compared.

\*\* This is the trivial case where all weights are zero.



Experiments were carried out on the images of the Yale Face Database [14]. The database consists of 15 different subjects that show eight different gestures. It was the goal to recognize each subject independent of the gesture. To achieve this we trained a wavelet networks for each individual where the training was done on the image showing the “normal” expression. We thus ended up with 15 different wavelet networks or, respectively, with 15 different operators  $\mathcal{T}_{\Psi_i}$ ,  $i = 1, \dots, 15$ . In fig. 7 and 8, example results (bottom rows) of the operator application  $\mathcal{T}_{\Psi_{01}}^{(J)}(J)$  on the different gestures and subjects (top rows) are shown. The wavelet network applied is “subject01”, the one in fig. 1, left, or, respectively, the very left one in fig. 7. The greater the difference between the original image and operator result of  $\mathcal{T}^{\mathcal{P}}$ , the less is the similarity and the less is the probability that the test image and the training image show the same subject. This can clearly be seen in the two sample figures. Whereas in fig. 7, the similarity is always good, the operator results of  $\mathcal{T}^{\mathcal{P}}$  in fig. 8 are all bad. Table 3 shows the computing results of the distance  $d_{\Psi}$  on the images of the database.

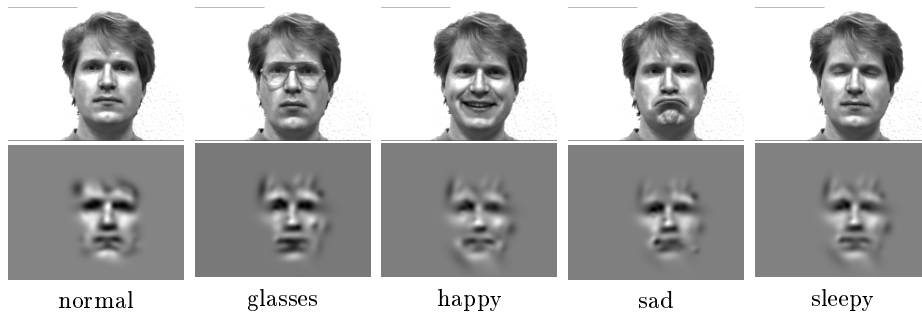


**Fig. 7.** Various images of “subject01” (top) and the results of the application of the operator  $\mathcal{T}_{\Psi}^{\mathcal{P}(g)}(g)$ . (bottom). To calculate these examples, the GWN of fig. 1,  $\hat{I}_{4,6}$ , with 52 wavelets was applied. The “normal” image was taken to be the training image  $f$ .

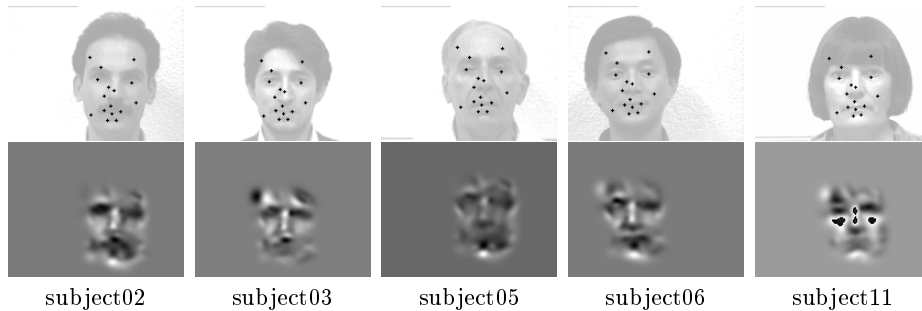


**Fig. 8.** Various subjects of the database (top) and the results of the application of the operator  $\mathcal{T}_{\Psi}^{\mathcal{P}(g)}(g)$ (bottom). To calculate these examples, the GWN of fig. 1,  $\hat{I}_{4,6}$ , with 52 wavelets was applied. The “normal” image in fig. 7 was taken to be the training image  $f$ .

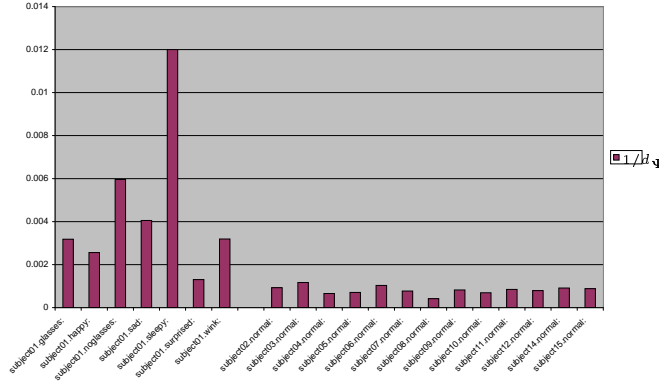


**Fig. 9.** The table shows the distance measurements  $1/d_{\Psi}$  of the images of the various subjects in the face database to the reference image in fig. 7, left. Higher values indicate a higher similarity between the two compared images. One sees that the values in the left part of the tables (same subject) indicate a much higher similarity than the values in the right part of the table (different subjects).

The results of table 3 show a clear difference for  $d_{\Psi}$  between probe images that show the original subject with different gestures and probe images that show other subjects. With this we reached a final recognition rate of 96% on the Yale Face Database [14]. See [1] for a comparison with other approaches.

With minor algebraic transformations, eq. (8) can be rewritten such that the distance  $d_{\Psi}$  can be written solely on the basis of the computed weight vectors:

$$d_{\Psi}(f, g) = (\mathbf{v} - \mathbf{w})^t (\Psi_{i,j}) (\mathbf{v} - \mathbf{w}),$$

where  $\mathbf{v}$  and  $\mathbf{w}$  is the weight vector with respect to  $\Psi$  of  $f$  and of  $g$ , respectively. The matrix  $(\Psi_{i,j}) = (\langle \psi_i, \psi_j \rangle)$  is the same above in section 2.1.

## 4 Conclusions

In this paper we introduced as the major contribution the Gabor wavelet network for object and image representation. We gave an overview of several experiments in order to show that the GWN is indeed a representation that is able to preserve a maximum of image information because it reflects precisely the properties of an object by a careful selection of wavelet parameters. The use of low-frequential Gabor functions ensures robustness to minor local changes. As a nice side effect, GWNs achieve a great data reduction. For example, in all our experiments we used for each GWN 52 wavelets, each defined by 5 parameters, so that each GWN needed an amount of 1040 bytes of memory. Our experimental results are quite promising. In fact, they show quite impressively that it is important for an object representation to reflect the specific individual properties of the object class that should be represented. This ensures that different individuals can be distinguished effectively independent from their gesture. The experiments were

carried out on a small face database and a generalization to larger databases is difficult.

**Acknowledgment** The images used are derived from the Yale Face Database. We thank T. Bülow and N. Krüger for valuable discussions.

## References

1. P.N. Belhumeur, J.P. Hespanha, and D.J. Kriegman. Eigenfaces vs. fisherfaces: Recognition using class specific linear projection. *IEEE Trans. Pattern Analysis and Machine Intelligence*, 19(7), 1997.
2. I. Daubechies. The wavelet transform, time-frequency localization and signal analysis. *IEEE Trans. Informat. Theory*, 36, 1990.
3. J. Daugman. Complete discrete 2D Gabor transform by neural networks for image analysis and compression. *IEEE Trans. Acoustics, Speech, and Signal Processing*, 36(7):1169–1179, 1988.
4. G. H. Granlund. From multidimensional signals to the generation of responses. In G. Sommer and J.J. Koenderink, editors, *Algebraic Frames for the Perception-Action Cycle*, pages 29–53, Int. Workshop, AFPAC'97, Kiel, Germany, September, 1997.
5. V Krüger, Sven Bruns, and G. Sommer. Efficient head pose estimation with gabor wavelet networks. In *Proc. British Machine Vision Conference*, Bristol, UK, Sept. 12-14, 2000. accepted for oral presentation.
6. V Krüger and G. Sommer. Affine real-time face tracking using gabor wavelet networks. In *Proc. Int. Conf. on Pattern Recognition*, Barcelona, Spain, Sept. 3-8, 2000. accepted for oral presentation.
7. V Krüger and G. Sommer. Gabor wavelet networks for object representation. In *Deutsche Arbeitsgemeinschaft für Mustererkennung*, 22. DAGM-Symposium, Kiel, Sept. 13-15, 2000. accepted for presentation.
8. T. S. Lee. Image representation using 2D Gabor wavelets. *IEEE Trans. Pattern Analysis and Machine Intelligence*, 18(10):959–971, 1996.
9. B.S. Manjunath and R. Chellappa. A unified approach to boundary perception: edges, textures, and illusory contours. *IEEE Trans. Neural Networks*, 4(1):96–107, 1993.
10. B. Moghaddam and A. Pentland. Probabilistic visual learning for object detection. *IEEE Trans. Pattern Analysis and Machine Intelligence*, 17(7):696–710, Juli 1997.
11. W.H. Press, B.P. Flannery, S.A. Teukolsky, and W.T. Vetterling. *Numerical Recipes, The Art of Scientific Computing*. Cambridge University Press, Cambridge, UK, 1986.
12. H. Szu, B. Telfer, and S. Kadambe. Neural network adaptive wavelets for signal representation and classification. *Optical Engineering*, 31(9):1907–1961, 1992.
13. L. Wiskott, J. M. Fellous, N. Krüger, and C. v. d. Malsburg. Face recognition by elastic bunch graph matching. *IEEE Trans. Pattern Analysis and Machine Intelligence*, 19(7):775–779, July 1997.
14. Yale University. Yale face database. <http://cvc.yale.edu/projects/yalefaces/yalefaces.html>, 1997.
15. Q. Zhang and A. Benviste. Wavelet networks. *IEEE Trans. Neural Networks*, 3(6):889–898, Nov. 1992.